

DMRG study of exciton condensation in the extended Falicov-Kimball model

P. Farkašovský

Institute of Experimental Physics, Slovak Academy of Sciences, Watsonova 47, 043 53 Košice, Slovakia

Received May 15, 2020, in final form August 13, 2020

The formation and condensation of excitonic bound states of conduction-band electrons and valence-band holes surely belongs to one of the most exciting ideas of contemporary solid state physics. In this short review we present the latest progress in this field reached by the density-matrix-renormalization-group (DMRG) calculations within various extensions of the Falicov-Kimball model. Particular attention is paid to a description of crucial mechanisms (interactions) that affect the stability of the excitonic phase, and namely: (i) the interband d - f Coulomb interaction, (ii) the f -electron hopping, (iii) the nonlocal hybridization with odd and even parity, (iv) combined effects of the local and nonlocal hybridization, (v) the nearest-neighbor Coulomb interaction between d and f electrons and (vi) the correlated hopping. The relevance of numerical results obtained within different extensions of the Falicov-Kimball model for a description of the real d - f materials is widely discussed.

Key words: Falicov-Kimball model, quantum condensates, one-dimensional systems

1. Introduction

The formation of excitonic quantum condensates is an intensively studied continuous problem in condensed matter physics [1–4]. Whilst theoretically predicted a long time ago [5], no conclusive experimental proof of the existence of the excitonic condensation has been achieved yet. However, the latest experimental studies of materials with strong electronic correlations showed that promising candidates for the experimental verification of the excitonic condensation could be $\text{TmSe}_{0.45}\text{Te}_{0.55}$ [6, 7], $1T\text{-TiSe}_2$ [8–11], Ta_2NiSe_5 [12], or a double bilayer graphene system [13]. In this regard, the mixed valence compound $\text{TmSe}_{0.45}\text{Te}_{0.55}$ was argued to exhibit a pressure-induced excitonic instability, related to an anomalous increase in the electrical resistivity [6, 7]. In particular, detailed studies of the pressure-induced semiconductor-semimetal transition in this material [based on the Hall effect, electrical and thermal (transport) measurements] showed that excitons are created in a large quantity and condense below 20 K. On the other hand, in the layered transition-metal dichalcogenide $1T\text{-TiSe}_2$, a BCS-like electron-hole pairing was considered as the driving force for the periodic lattice distortion [8–11]. Moreover, quite recently, the excitonic-insulator state was probed by angle-resolved photoelectron spectroscopy in the semiconducting Ta_2NiSe_5 compound [12]. These results have stimulated further experimental and theoretical studies with regard to the formation and possible condensation of excitonic bound states of electron and holes in correlated systems. At present, it is generally accepted that the minimal theoretical model for a description of excitonic correlations in these materials could be the Falicov-Kimball model [14] and its extensions which were successfully used in the past years to test the exciting idea of electronic ferroelectricity [15–25] that is directly related with the formation of an excitonic insulator [26–35]. In its original form, the Falicov-Kimball model describes a two-band system of localized f electrons and itinerant d electrons with short-ranged f - d Coulomb interaction U :

$$H_0 = \sum_{ij} t_{ij} d_i^\dagger d_j + U \sum_i f_i^\dagger f_i d_i^\dagger d_i + E_f \sum_i f_i^\dagger f_i, \quad (1.1)$$

where f_i^+ , f_i are the creation and annihilation operators for an electron in the localized state at lattice site i with the binding energy E_f and d_i^+ , d_i are the creation and annihilation operators of the itinerant spinless electrons in the d -band Wannier state at site i .

The first term of (1.1) is the kinetic energy corresponding to quantum-mechanical hopping of the itinerant d electrons between sites i and j . These intersite hopping transitions are described by the matrix elements t_{ij} , which are $-t_d$ if i and j are the nearest neighbors and zero otherwise (in what follows all parameters are measured in units of t_d). The second term represents the on-site Coulomb interaction between the d -band electrons with density $n_d = \frac{1}{L} \sum_i d_i^+ d_i$ and the localized f electrons with density $n_f = \frac{1}{L} \sum_i f_i^+ f_i$, where L is the number of lattice sites. The third term stands for the localized f electrons whose sharp energy level is E_f .

Since in this simple model, the local occupation number $f_i^+ f_i$ commutes with the total Hamiltonian of the system, the local f -electron number is a strictly conserved quantity and thus the d - f electron coherence cannot be established in such a system. If hybridization $H_V = V \sum_i d_i^+ f_i + f_i^+ d_i$ between both bands is included, the f charge occupation is no longer a good quantum number, and it is possible to build coherence between d and f electrons. Hybridization between the itinerant d and localized f states, however, is not the only way to develop d - f coherence. Theoretical works of Batista et al. [22, 23] showed that the ground state with a spontaneous electric polarization can also be induced by the nearest-neighbor f -electron hopping $H_{t_f} = -t_f \sum_{\langle i,j \rangle} f_i^+ f_j$, but only for dimensions $D > 1$. In the strong coupling limit, this result was proven by mapping the extended Falicov-Kimball model into the xxz spin 1/2 model with a magnetic field along the z -direction, while in the intermediate coupling regime the ferroelectric state was identified numerically by constrained path Monte Carlo (CPMC) technique. Based on these results, the authors postulated the following conditions that favour the formation of the electronically driven ferroelectric state: (a) The system must be in a mixed-valence regime and the two bands involved must have different parity. (b) It is best, though not necessary, if both bands have similar bandwidths. (c) A local Coulomb repulsion (U) between the different orbitals is required.

Later on this model was extensively used to describe different phases in the ground state and special properties of the excitonic phase [26–32]. It was found that the ground state phase diagram exhibits a very simple structure consisting of only four phases, and namely, the full d and f band insulator (BI), the excitonic insulator (EI), the charge-density-wave (CDW) and the staggered orbital order (SOO). The EI is characterized by a nonvanishing $\langle d^+ f \rangle$ average. The CDW is described by a periodic modulation in the total electron density of both f and d electrons, and the SOO is characterized by a periodic modulation in the difference between the f and d electron densities.

In this article we focus our attention on the properties of the EI phase induced by local hybridization V in the one dimension. Although it is generally known that there is no nonvanishing $P_{df} = \langle d^+ f \rangle$ expectation value in the limit of vanishing hybridization (no spontaneous hybridization), the studies that we performed in the past years on various extensions of the original Falicov-Kimball model showed that it is possible to dramatically enhance excitonic correlations in the limit of small, but finite V by additional interactions/factors [36–39]. The effects of most important interactions are discussed in this review. In particular, there are: (i) the interband d - f Coulomb interaction, (ii) the f -electron hopping, (iii) the nonlocal hybridization with odd and even parity, (iv) combined effects of the local and nonlocal hybridization, (v) the nearest-neighbor Coulomb interaction between d and f electrons and (vi) the correlated hopping. The main goal of this review is not to examine the possibilities of spontaneous symmetry breaking (a spontaneous hybridization) in various extensions of the Falicov-Kimball model, but to show how these extensions (different interaction terms) influence the properties of the excitonic phase induced by local hybridization. All presented results were obtained within the density-matrix-renormalization-group (DMRG) method, where we typically keep up to 500 states per block, although in the numerically more difficult cases (where the DMRG results converge slower), we keep up to 1000 states. Truncation errors [40], given by the sum of the density matrix eigenvalues of the discarded states, vary from 10^{-6} in the worse cases to zero in the best cases.

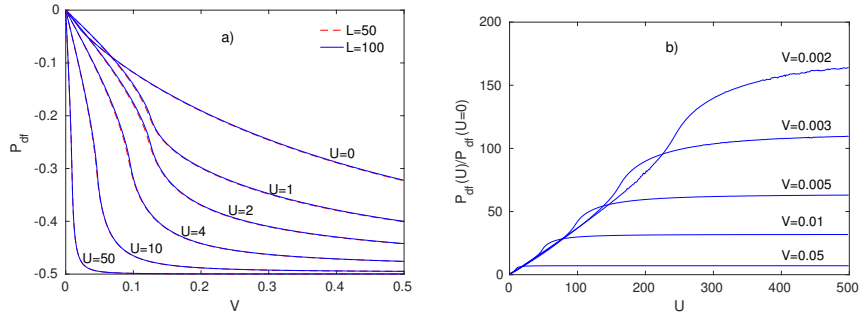


Figure 1. (Colour online) a) The hybridization dependence of the d - f -excitonic average $P_{df} = \langle d_i^+ f_i \rangle$ in the extended Falicov-Kimball model calculated for six different values of U and two different values of L . The symmetric case $E_f = 0$. b) The ratio of the interacting $P_{df}(U)$ and non-interacting $P_{df}(U = 0)$ excitonic average as a function of U calculated for several selected values of local hybridization V on the cluster of $L = 100$ sites [36].

2. Results and Discussion

2.1. Effects of interband Coulomb interaction

Let us start our review with the discussion of effects of the Coulomb interactions [36]. In this case, Hamiltonian consists of two terms: H_0 , which is given by (1.1) and $H_V = V \sum_i d_i^+ f_i + f_i^+ d_i$. Our DMRG results obtained for the symmetric case $E_f = 0$ are summarized in figure 1 a and in figure 1 b where the $P_{df} = \langle d_i^+ f_i \rangle$ expectation value is shown as a function of hybridization for several values of Coulomb interaction U (figure 1 a) and the ratio $\Delta = P_{df}(U)/P_{df}(U = 0)$ for several values of V (figure 1 b). Figure 1 a clearly demonstrates that there is no nonvanishing $\langle d^+ f \rangle$ -expectation value in the limit of vanishing hybridization for all examined values of U . At the same time, these data reveal an important feature of the model and namely that the P_{df} expectation value is dramatically enhanced with increasing U in comparison to the noninteracting case. This is explicitly shown in figure 1 b where the ratio of the interacting $P_{df}(U)$ and non-interacting $P_{df}(U = 0)$ excitonic average is plotted for several selected values of hybridization. For all examined values of V , the ratio $\Delta = P_{df}(U)/P_{df}(U = 0)$ rapidly increases with increasing interband Coulomb interaction U from its initial value $\Delta = 1$ to its saturated value $\Delta = \Delta_s$ that also dramatically increases with a decreasing V . Indeed, while $\Delta_s \sim 7$ for $V = 0.05$ its value increases up to ~ 200 for $V = 0.002$. This result is very important from the point of view of real rare-earth materials with d and f electrons. In these materials the local hybridization is usually forbidden due to the crystal symmetry and thus the $d - f$ coherence cannot be established. However, according to our results, any infinitesimal hybridization, induced by some additional mechanism, could lead to a robust excitonic average due to the interband Coulomb interaction. Such an additional mechanism could be, for example, the electron-phonon interaction H_{el-ph} that can be reduced to the phonon-mediated local hybridization (electron-electron interactions) by the standard canonical transformation of the form $e^S H e^{-S}$, where the operator S is determined so that $H_{el-ph} = -[S, H_{loc}]$ and H_{loc} are all local terms corresponding to f , d electrons and phonons [41].

To examine the nature of the EI state more in detail, we have calculated, in accordance with [31] and [32], the exciton-exciton correlation function $\langle b_i^+ b_j \rangle$ with $b_i^+ = d_i^+ f_i$ and the excitonic momentum distribution $N(q) = \langle b_q^+ b_q \rangle$ with $b_q^+ = (1/\sqrt{L}) \sum_k d_{k+q}^+ f_k$. We have found that the exciton-exciton correlation function $\langle b_i^+ b_j \rangle$ exhibits power-law correlations $|i - j|^{-\alpha}$ (with α between 3 and 4) and the excitonic momentum distribution $N(q)$ diverges for $q = 0$ (see figure 2 a), signaling a Bose-Einstein condensation of preformed excitons. Moreover, figure 2b shows that the density of zero momentum excitons $n_0 = \frac{1}{L} N(q = 0)$ as well as the total exciton density $n_T = \frac{1}{L} \sum_q N(q)$ strongly depend on the values of the Coulomb interaction U and that already for relatively small values of U ($U \sim 4$) practically all particles are paired in electron-hole pairs with significant fraction of $n_0/n_T \sim 0.5$ excitons in the zero-momentum state.

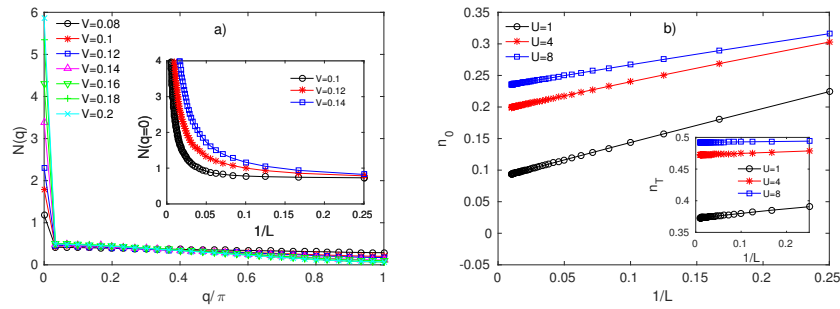


Figure 2. (Colour online) a) The excitonic momentum distribution $N(q)$ calculated for different values of V at $U = 1$, $E_f = 0$ and $L = 60$. The inset shows a divergence of $N(q = 0)$ for $L \rightarrow \infty$ for three selected values of V . b) The density of zero momentum excitons n_0 and the total exciton density n_T as functions of $1/L$ calculated for several different values of U at $V = 0.2$ and $E_f = 0$ [36].

2.2. Effects of f -electron hopping

With regard to the situation in real materials, where there always exists a finite overlap of f orbitals on the neighbouring sites, it is interesting to ask what happens if the f -electron hopping $H_{t_f} = -t_f \sum_{\langle i,j \rangle} f_i^+ f_j$ is also taken into account [37]. In accordance with some previous theoretical studies, which documented strong effects of the parity of f band on the stability of the excitonic phase [22, 23], we have examined the model for both the positive (the even parity) and negative (the odd parity) values of the f -electron hopping integrals t_f . The results of our non-zero t_f DMRG calculations for n_0 are displayed in figure 3 and they clearly demonstrate that the zero-momentum condensate is suppressed in the limit of positive values of t_f , while it remains robust for negative values of t_f . This

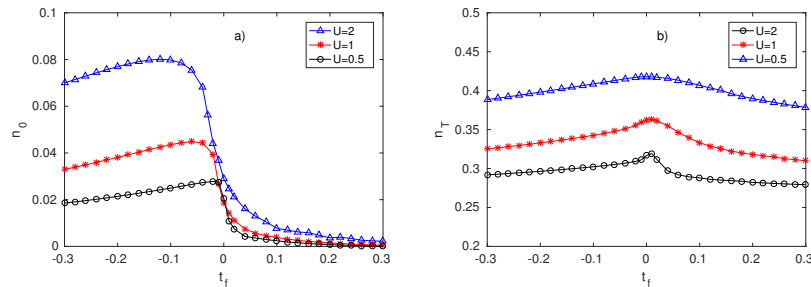


Figure 3. (Colour online) n_0 (a) and n_T (b) as functions of t_f calculated for three different values of U ($E_f = 0$, $V = 0.1$, $L = \infty$) [37].

result is intuitively expected since our previous Hartree-Fock (HF) results [24] showed that only the negative values of t_f stabilize the ferroelectric phase, while the positive values stabilize the antiferroelectric phase. The effect of t_f is especially strong for U small (see figure 3 a), where continuous but very steep changes of n_0 are observed for $t_f \rightarrow 0^+$. On the contrary, the total exciton density n_T (figure 3 b) exhibits only a weak dependence on the f -electron hopping parameter t_f , over the whole interval of t_f values.

2.3. Effects of f -level position (pressure)

So far we have presented the results exclusively for $E_f = 0$. Let us now briefly discuss the effect of the change of the f -level position [37]. This study is also interesting from the point of view that taking into account the parametrization between the external pressure and the position of the f level ($E_f \sim p$), one can also deduce, at least qualitatively, their p dependences from the E_f dependences of the ground

state characteristics [42]. The resultant E_f dependences of the density of zero momentum excitons n_0 are shown in figure 4 a for several values of V and $U = 0.5$. One can see that the density of zero

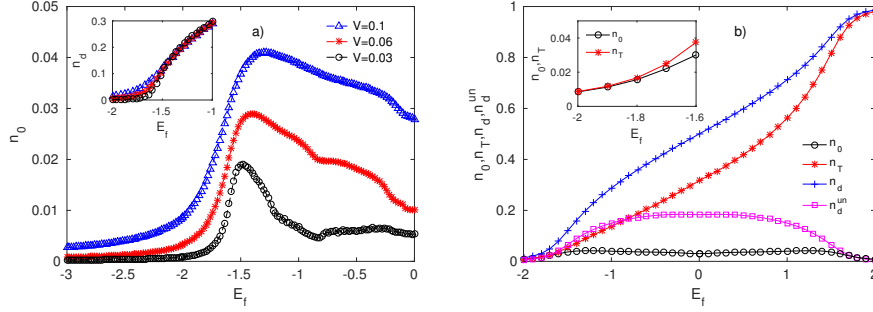


Figure 4. (Colour online) a) n_0 as a function of E_f calculated for three different values of V ($t_f = 0, U = 0.5, L = \infty$). The inset shows the density of d electrons n_d near $E_f = -1.5$. b) n_0, n_T, n_d and $n_d^{\text{un}} = n_d - n_T$ as functions of E_f calculated for $t_f = 0, U = 0.5, V = 0.1$ and $L = \infty$. The inset shows the behaviour of n_0 and n_T near $E_f = -2$ [37].

momentum excitons is nonzero over the whole interval of E_f values. Moreover, we have found that the values of n_0 are extremely enhanced in the region near $E_f \sim -1.5$, which is obviously due to a significant enhancement of the d electron population in the d band (see the inset in figure 4 a).

To describe the process of formation of excitonic bound states with increasing E_f more in detail, we have also plotted in figure 4 b, besides the density of zero momentum excitons n_0 , the total exciton density n_T , the total d -electron density n_d and the total density of unbond d electrons $n_d^{\text{un}} = n_d - n_T$. It is seen (see the inset in figure 4 b) that below $E_f \sim -1.8$, n_0 and n_T coincides, which means that the excitonic insulator in this region is practically completely driven by the condensation of zero-momentum excitons. Above this value n_T starts to sharply increase, while n_0 tends to its maximum at $E_f \sim -1.3$ and then gradually decreases to its minimum at $E_f = 0$. Similar behaviour with increasing E_f also exhibits the density of unbond d electrons n_d^{un} , though the values of n_d^{un} are several times larger than n_0 . It is interesting to note that although the total exciton density n_T increases over the whole interval of E_f values, the number of unbond d electrons remains practically unchanged over the wide range of E_f values (from $E_f = -1$ to $E_f = 1$), since its decrease, due to the formation of excitonic pairs, is compensated by the increase of $n_d(E_f)$. Thus, we can conclude that in the pressure induced case, when the f -level energy shifts up with the applied pressure [42], the model is capable of describing, at least qualitatively, the increase in the total density of excitons with external pressure and the increase or decrease (according to the initial position of E_f at ambient pressure) in the n_0 and n_d^{un} .

2.4. Effects of non-local hybridization with inversion symmetry

As already mentioned, from the physics viewpoint, the most interesting case corresponds to the case of finite non-local hybridization [37]. The importance of this term emphasizes the fact that the on-site hybridization V is usually forbidden in real d - f systems for parity reasons. Instead of the on-site hybridization, one should consider in these materials the non-local hybridization with inversion symmetry $V_{i,j} = V_{\text{non}}(\delta_{j,i-1} - \delta_{j,i+1})$ which leads to k -dependent hybridization of the opposite parity that corresponds to the d band [$V_k \sim \sin(k)$] [43]. Typical examples of $1/L$ dependence of the excitonic momentum distribution $N(q = 0)$ obtained for three representative values of the interband Coulomb interaction and two values of f -electron hopping are displayed in figure 5 a and figure 5 b. These results clearly demonstrate that there is no sign of divergence in the $1/L$ -dependence of $N(0)$ neither for $t_f = 0$ nor for $t_f = -0.05$ and thus, there is no signal of forming the Bose-Einstein condensate in the presence of non-local hybridization with the inversion symmetry. Thus, our results indicate that the class of possible candidates for the appearance of the Bose-Einstein condensation of excitons in real d - f materials is strongly limited, since the local hybridization is usually forbidden in these systems for parity

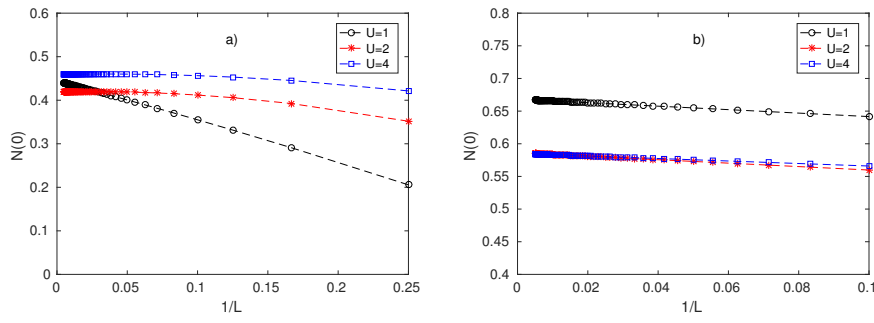


Figure 5. (Colour online) $N(0)$ as a function of $1/L$ calculated for three different values of U and two different values of t_f : a) $t_f = 0$, b) $t_f = -0.5$ ($E_f = 0, V_{\text{non}} = 0.1$) [37].

reasons and the non-local hybridization with the inversion symmetry does not support the formation of the Bose-Einstein condensate.

2.5. Combined effects of local and non-local hybridization with equal parity of d and f orbitals

In this situation, the most promising candidates for studying this phenomenon seem to be the systems with equal parity of d and f orbitals, where the nonlocal hybridization H_n can be written as [38]:

$$H_n = V_n \sum_{\langle i,j \rangle} (d_i^+ f_j + H.c.). \quad (2.1)$$

In such systems, the local hybridization V is allowed, and thus one can examine the combined effects of the local and nonlocal hybridization within the unified picture. In the weak ($U < 1$) and strong ($V \ll U$ and $V_n \ll U$) coupling limits, the model Hamiltonian $H_0 + H_V + H_n$ was recently analyzed by Zenker et al. in [44], and the corresponding mean-field quantum phase diagrams were presented as functions of the model parameters U, V, V_n and E_f for the half-filled band case $n_f + n_d = 1$ and $D = 2$. Moreover, examining the effects of the local V and nonlocal V_n hybridization, they found that in the pseudospin space ($c_{i\uparrow}^+ = d_i^+, c_{i\downarrow}^+ = f_i^+$), the nonlocal hybridization V_n favors the staggered Ising-type ordering along the x direction, while V favors a uniform polarization along the x direction and the staggered Ising-type ordering along the y direction. In our paper [38] we have examined the model for arbitrary V and V_n and unlike the paper of Zenker et al. [44] we have focused our attention primarily on a description of process of formation and condensation of excitonic bound states.

Let us discuss the results obtained for $n_0 = \frac{1}{L}N(q=0)$, $n_\pi = \frac{1}{L}N(q=\pi)$, n_d and n_d^{un} as functions of the f -level position E_f which can give us, at least qualitatively, the answer to the very important question, and namely, how these quantities change with the applied pressure p . In figure 6 we present the resultant behaviours of $n_0, n_\pi, n_d, n_d^{\text{un}}$ as functions of the f -level position E_f obtained by the DMRG method for $V = 0.2$ and several different values of V_n . In all examined cases, the density of zero-momentum excitons is the most significantly enhanced for d -electron densities near the half-filled band case $E_f = 0$ and $n_d = 1/2$. The changes of n_0 are gradual for $E_f < 0$ and very steep, but still continuous, for $E_f > 0$. The fully different behaviour exhibits the density of π -momentum excitons n_π . Its enhancement with increasing E_f is practically negligible for $E_f < 0$, but from this value n_π it starts to sharply increase and tends to its saturation value corresponding to the fully occupied d band $n_d \sim 1$. The density of unbound d electrons n_d^{un} exhibits a very simple behaviour for $E_f < 0$. In this limit, n_d^{un} gradually increases with increasing E_f for all examined values of nonlocal hybridization V_n . However, in the opposite case ($E_f > 0$), the density of unbound d electrons n_d^{un} behaves fully differently for $V_n < V_n^c$ and $V_n > V_n^c$, where $V_n^c \sim 0.2$. For $V_n < V_n^c$, the density of unbound d electrons n_d^{un} gradually decreases with an increasing E_f and tends to zero when E_f approaches the upper edge of the noninteracting band $E_f = 2$, but in the opposite limit the density of unbound d electrons n_d^{un} decreases by the interval of E_f values from $E_f = 0$ to $E_f^c(V_n)$, and

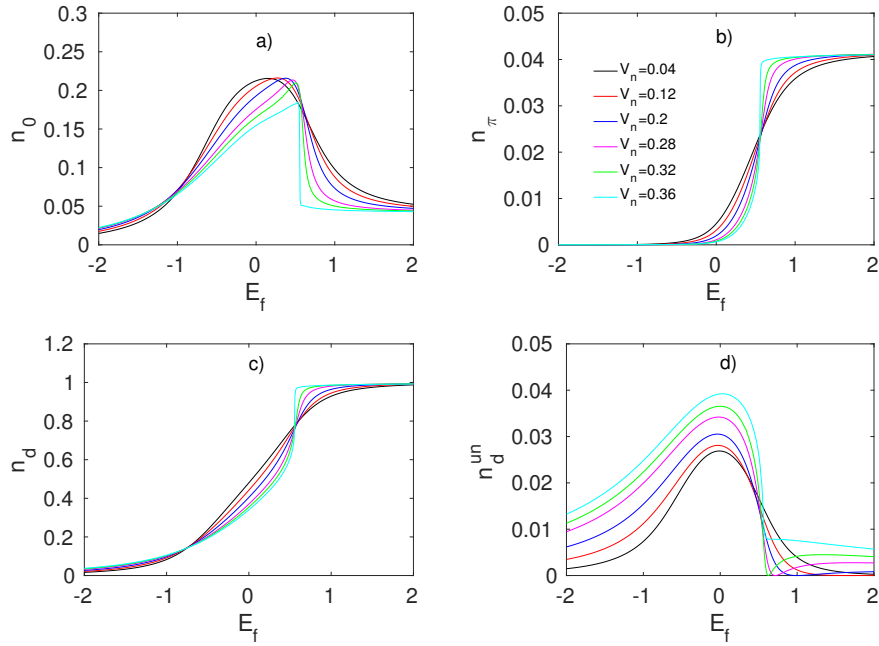


Figure 6. (Colour online) The density of zero-momentum excitons n_0 (a), the density of π -momentum excitons n_π (b), the total d -electron density n_d (c), and the total density of unbound d electrons $n_d^{\text{un}} = n_d - n_T$ (d) as functions of E_f calculated for $U = 4, V = 0.2, L = 60$ and six different values of V_n [38].

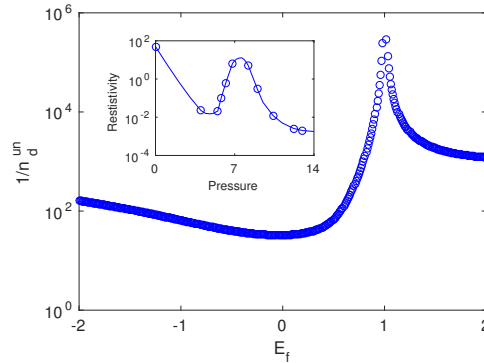


Figure 7. (Colour online) The inverse value of the density of unbound d -electrons n_d^{un} as a function of the f -level energy E_f calculated for $U = 4, V = 0.2, V_n = 0.2$ and $L = \infty$ [38]. The inset shows the resistivity as the function of pressure in $\text{TmSe}_{0.45}\text{Te}_{0.55}$ at 4.2 K [6].

n_d^{un} starts to increase again for $E_f > E_f^c(V_n)$. Taking into account the above mentioned parametrization between E_f and the external pressure p , as well as the fact that the electrical conductivity is proportional to the density of unbound electrons n_d^{un} (and the electrical resistivity to $1/n_d^{\text{un}}$), the results discussed above could have very important physical consequences. Indeed, in figure 7 we have plotted the quantity $1/n_d^{\text{un}}$ (in the logarithmic scale) as a function of E_f and compare it with experimental measurements of the pressure dependence of the electrical resistivity in the mixed valence compound $\text{TmSe}_{0.45}\text{Te}_{0.55}$ (see the inset in figure 7). One can see that there is a nice qualitative accordance between our theoretical predictions and experimental results of Wachter et al. [6]. In spite of the fact that our model is in many aspects very simplified, the physics that could lead to the unusual behaviour of the

electrical resistivity in $\text{TmSe}_{0.45}\text{Te}_{0.55}$ under the external pressure seems to be clear. This is a result of the formation and condensation of excitonic bound states of conduction-band electrons and valence-band holes.

2.6. Effects of non-local Coulomb interactions

The above discussed results show that the Falicov-Kimball model has a great potential to describe some of the anomalous features of real complex materials such as rare-earth compounds. On the other hand, it should be noted that the original version of the model, as well as its extensions discussed above, represent a too crude approximation of real rare-earth compounds, since we neglect all nonlocal Coulomb interactions, that can change this picture. For a correct description of these materials one should take into account at least the following nonlocal Coulomb interaction terms [39]:

$$H_{\text{non}} = U_{dd} \sum_{\langle ij \rangle} n_i^d n_j^d + U_{df} \sum_{\langle ij \rangle} n_i^d n_j^f + U_{ff} \sum_{\langle ij \rangle} n_i^f n_j^f + U_{ch} \sum_{\langle ij \rangle} d_i^+ d_j (n_i^f + n_j^f), \quad (2.2)$$

which represent the nearest-neighbour Coulomb interaction between two d electrons (the first term), between one d and one f electron (the second term), between two f electrons (the third term) and the so-called correlated hopping (the last term).

There is a number of papers, where the influence of individual interaction terms from (2.2) on the ground state properties of the Falicov-Kimball model has been studied. However, there are only a few where the combined effects of two or three terms were considered. Among the papers dealing with the influence of individual interactions, let us mention the work [45] (and references therein) where the effects of nonlocal interaction between d and f electrons are examined and the excellent papers of Shvaika et al. [46–48] where rigorous results for the influence of the correlated hopping on the thermodynamical functions were derived within the local approach and then used for a description of various physical problems. Among the papers dealing with combined effects of two or three terms, let us mention the works [49, 50] (and references therein). From this point of view, the model Hamiltonian $H = H_0 + H_V + H_{\text{non}}$ considered here represents one of the most complex extensions of the Falicov-Kimball model used for a description of ground state properties of strongly correlated systems. Here, we focus our attention exclusively on a discussion of two main problems, and namely, the process of formation and condensation of excitonic bound states and the problem of valence transitions in the generalized Falicov-Kimball model. To simplify numerical calculations, we adopt here the following model $U_{dd} = U_{ff} = U_{df} = U_{nn}$, that allows us to reduce the number of model parameters and at the same time to keep all nonlocal interaction terms nonzero. The physically most interesting case corresponds to the situation where both (U_{nn} as well as U_{ch}) interactions are switched on simultaneously and numerical results for this case are summarized in figure 8. One can see that combined effects of non-local interactions lead to a number of interesting results: (i) strong suppression of the zero-momentum condensate in the region of E_f , where $n_d \sim 0.5$, (ii) stabilization of the intermediate phase with $n_d \sim 0.5$ for increasing $U_{nn} = U_{ch}$, (iii) strong enhancement of the total density of unbond d electrons n_d^{un} with an increase of $U_{nn} = U_{ch}$. (iv) stabilization of zero momentum condensate for some values of the f -level energy E_f in the weak coupling limit $U_{nn} = U_{ch} \sim 0.2$, (v) appearance of discontinuous valence transitions for sufficiently large values of $U_{nn} = U_{ch} \sim 0.4$ and (vi) discontinuous disappearance of the density of zero momentum excitons, as well as discontinuous changes in the total density of excitons n_T and the total density of unbond d electrons n_d^{un} at the valence transition points.

The appearance of discontinuous changes in some ground-state observables such as the density of conduction d (valence f) electrons, the density of zero-momentum condensate, the density of unbond electrons, is a very important result from the point of view of rare-earth compounds. In some of them, e.g., the mixed valence system SmS such discontinuous changes are experimentally observed in the density of valence electrons when the external hydrostatic pressure is applied [51], though they were not satisfactorily described so far. Indeed, as mentioned above, the SmS compound is a mixed valence system, with fluctuating valence and thus for its description one should take into account the hybridization between the localized f and conduction d electron states. However, more reliable methods, such as alloy-analog approximation [52], renormalization group method [53], exact diagonalization method [54], predict only

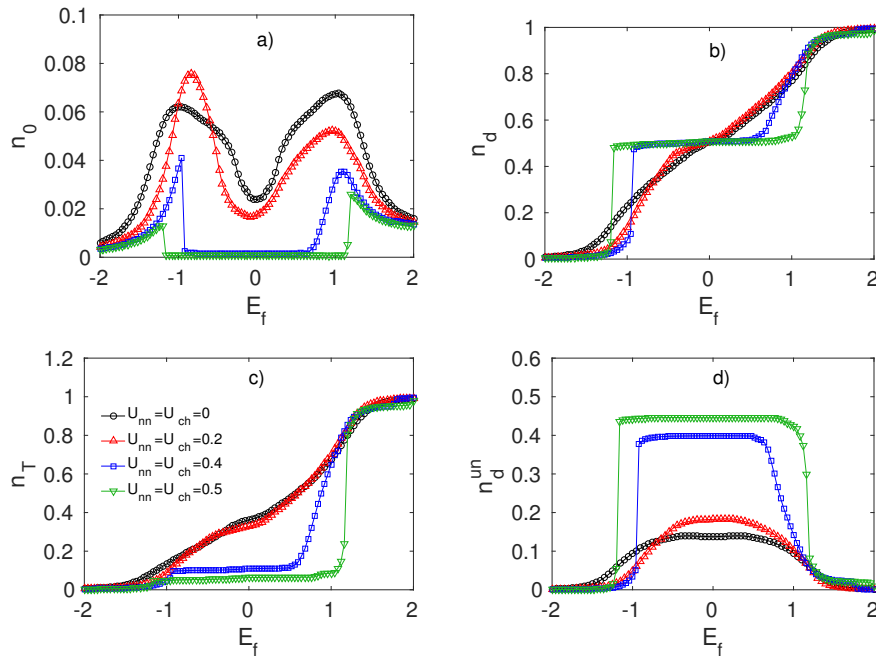


Figure 8. (Colour online) n_0 , n_d , n_T and $n_d^{\text{un}} = n_d - n_T$ as functions of E_f calculated for four different values of U_{ch} ($U_{ch} = 0, 0.2, 0.4, 0.5$) at $U_{nn} = U_{ch}$, $U = 1$, $V = 0.1$, $L = 100$ and $n_f + n_d = 1$ [39].

the continuous valence transitions within the Falicov-Kimball model extended by the local hybridization. Here, we show that considering the parametrization between the external pressure p and the f -level position E_f , the pressure induced discontinuous valence transitions are possible to generate also in such a system under a very realistic assumption, namely, that nonlocal interactions are switched on. This opens up a new route to the understanding of various ground-state anomalies observed in the rare-earth compounds within the unified picture.

Finally, it should be noted that although all the results presented in this review were obtained for the one-dimensional case, their validity is probably much more general. Indeed, a direct comparison of our one-dimensional DMRG and two dimensional Hartree-Fock results [37], obtained for the density of zero-momentum excitons as a function of t_f and E_f , revealed only a weak dependence of n_0 on the system dimension indicating a possible extension of our one-dimensional DMRG results to real two and three dimensional systems. Moreover, in the two-dimensional case, we can switch off completely the local hybridization, since in this case the excitonic condensate can be generated by other terms (the f -electron hopping), modelling more realistically the situation in rare-earth compounds.

Acknowledgements

This work was supported by projects VEGA 2-0112-18, APVV-17-0020, ITMS 2220120047, ITMS 26230120002 and IMTS 26210120002.

References

1. Blatt J.M., Böer K.W., Brandt W., Phys. Rev., 1962, **126**, 1691, doi:10.1103/PhysRev.126.1691.
2. Keldysh L.V., KopaeV H.Y.V., Sov. Phys. Solid State, 1965, **6**, 2219.
3. Moskalenko S.A., Snoko D.W., Bose-Einstein Condensation of Excitons and Biexcitons, Cambridge Univ. Press, Cambridge, 2000.

4. Littlewood P.B., Eastham P.R., Keeling J.M.J., Marchetti F.M., Simons D.B., Szymanska M.H., *J. Phys.: Condens. Matter*, 2004, **16**, S3597, doi:10.1088/0953-8984/16/35/003.
5. Des Cloizeaux J., *J. Phys. Chem. Solids*, 1965, **26**, 259, doi:10.1016/0022-3697(65)90153-8.
6. Neuenschwander J., Wachter P., *Phys. Rev. B*, 1990, **41**, 12693, doi:10.1103/PhysRevB.41.12693.
7. Bucher B., Steiner P., Wachter P., *Phys. Rev. Lett.*, 1991, **67**, 2717, doi:10.1103/PhysRevLett.67.2717.
8. Monney C., Monney G., Aebi P., Beck H., *Phys. Rev. B*, 2012, **85**, 235150, doi:10.1103/PhysRevB.85.235150.
9. Zenker B., Fehske H., Beck H., Monney C., Bishop A.R., *Phys. Rev. B*, 2013, **88**, 075138, doi:10.1103/PhysRevB.88.075138.
10. Monney G., Monney C., Hildebrand B., Aebi P., Beck H., *Phys. Rev. Lett.*, 2015, **114**, 086402, doi:10.1103/PhysRevLett.114.086402.
11. Watanabe H., Seki K., Yunoki S., *Phys. Rev. B*, 2016, **91**, 205135, doi:10.1103/PhysRevB.91.205135.
12. Wakisaka I., Sudayama T., Takubo K., Mizokawa T., Arita M., Namatame H., Taniguchi M., Katayama N., Nohara M., Takagi H., *Phys. Rev. Lett.*, 2009, **103**, 026402 doi:10.1103/PhysRevLett.103.026402.
13. Perali A., Neilson D., Hamilton A.R., *Phys. Rev. Lett.*, 2013, **110**, 146803, doi:10.1103/PhysRevLett.110.146803.
14. Falicov L.M., Kimball J.C., *Phys. Rev. Lett.*, 1969, **22**, 997, doi:10.1103/PhysRevLett.22.997.
15. Portengen T., Östreich T., Sham L.J., *Phys. Rev. Lett.*, 1996, **76**, 3384, doi:10.1103/PhysRevLett.76.3384.
16. Portengen T., Östreich T., Sham L.J., *Phys. Rev. B*, 1996, **54**, 17452, doi:10.1103/PhysRevB.54.17452.
17. Czycholl G., *Phys. Rev. B*, 1999, **59**, 2642, doi:10.1103/PhysRevB.59.2642.
18. Farkašovský P., *Phys. Rev. B*, 1999, **59**, 9707, doi:10.1103/PhysRevB.59.9707.
19. Farkašovský P., *Phys. Rev. B*, 2002, **65**, 81102, doi:10.1103/PhysRevB.65.81102.
20. Zlatić V., Freericks J.K., Lemanski R., Czycholl G., *Philos. Mag. B*, 2001, **81**, 1443, doi:10.1080/13642810110066470.
21. Freericks J.K., Zlatić V., *Rev. Mod. Phys.*, 2003, **75**, 1333, doi:10.1103/RevModPhys.75.1333.
22. Batista C.D., *Phys. Rev. Lett.*, 2002, **89**, 166403, doi:10.1103/PhysRevLett.89.166403.
23. Batista C.D., Gubernatis J.E., Bonča, Lin H.Q., *Phys. Rev. Lett.*, 2004, **92**, 187601, doi:10.1103/PhysRevLett.92.187601 .
24. Farkašovský P., *Phys. Rev. B*, 2008, **77**, 155130, doi:10.1103/PhysRevB.77.155130.
25. Schneider C., Czycholl, *Eur. Phys. J. B*, 2008, **64**, 43, doi:10.1140/epjb/e2008-00273-y.
26. Zenker B., Ihle D., Bronold F.X., Fehske H., *Phys. Rev. B*, 2010, **81**, 115122, doi:10.1103/PhysRevB.81.115122.
27. Phan V.N., Becker K.W., Fehske H., *Phys. Rev. B*, 2010, **81**, 205117, doi:10.1103/PhysRevB.81.205117.
28. Seki K., Eder R., Ohta Y., *Phys. Rev. B*, 2011, **84**, 245106, doi:10.1103/PhysRevB.84.245106.
29. Zenker B., Ihle D., Bronold F.X., Fehske H., *Phys. Rev. B*, 2012, **85**, 121102R, doi:10.1103/PhysRevB.85.121102.
30. Kaneko T., Seki K., Ohta Y., *Phys. Rev. B*, 2012, **85**, 165135, doi:10.1103/PhysRevB.85.165135.
31. Kaneko T., Ejima S., Fehske H., Ohta Y., *Phys. Rev. B*, 2013, **88**, 035312, doi:10.1103/PhysRevB.88.035312.
32. Ejima S., Kaneko T., Ohta Y., Fehske H., *Phys. Rev. Lett.*, 2014, **112**, 026401, doi:10.1103/PhysRevLett.112.026401.
33. Apinyan V., Kopeck T.K., *J. Low Temp. Phys.*, 2014, **176**, 27, doi:10.1007/s10909-014-1165-x.
34. Kuneš J., *J. Phys.: Condens. Matter*, 2015, **27**, 333201, doi:10.1088/0953-8984/27/33/333201.
35. Golosov D.I., *Phys. Rev.*, 2020, **101**, 165130, doi:10.1103/PhysRevB.101.165130.
36. Farkašovský P., *EPL*, 2015 **110**, 47007 doi:10.1209/0295-5075/110/47007.
37. Farkašovský P., *Phys. Rev. B*, 2017 **95**, 045101, doi:10.1103/PhysRevB.95.045101.
38. Farkašovský P., *Solid State Commun.*, 2017, **255**, 24, doi:10.1016/j.ssc.2017.03.005.
39. Farkašovský P., Regeciová L., *Eur. Phys. J. B*, 2019, **92**, 141, doi:10.1140/epjb/e2019-90406-6.
40. White S.R., *Phys. Rev. Lett.*, 1992, **69**, 2863, doi:10.1103/PhysRevLett.69.2863.
41. Brouers F., de Menezes O.L.T., *Phys. Status Solidi B*, 1981, **104**, 541, doi:10.1002/pssb.2221040218.
42. Gonçalves da Silva C.E.T., Falicov L.M., *Solid State Commun.*, 1975, **17**, 1521, doi:10.1016/0038-1098(75)90986-2.
43. Czycholl G., *Phys. Rep. B*, 1986, **143**, 277, doi:10.1016/0370-1573(86)90177-8.
44. Zenker B., Fehske H., Batista C.D., *Phys. Rev. B*, 2010, **82**, 165110, doi:10.1103/PhysRevB.82.165110.
45. Farkašovský P., *Acta Phys. Slovaca*, 2010, **60**, 497, doi:10.2478/v10155-010-0005-z.
46. Shvaika A.M., *Phys. Rev. B*, 2003, **67**, 075101, doi:10.1103/PhysRevB.67.075101.
47. Shvaika A.M., *Condens. Matter Phys.*, 2014, **17**, 43704, doi:10.5488/CMP.17.43704.
48. Dobushovskiy D.A., Shvaika A.M., Zlatić V., *Phys. Rev. B*, 2017, **95**, 125133, doi:10.1103/PhysRevB.95.125133.
49. Čenčariková H., Farkašovský P., Žonda M., *Acta Phys. Pol. A*, 2008, **113**, 287, doi:10.12693/APhysPolA.113.287.
50. Lemański R., Kapcia K.J., Robaszkiewicz S., *Phys. Rev. B*, 2017, **96**, 205102, doi:10.1103/PhysRevB.96.205102.
51. Rohler J., *Handbook on the Physics and Chemistry of Rare Earths*, Vol. 10, Gschneider K.A., Eyring L.R.,

- Huffner S. (Eds.) Amsterdam: North-Holland, 453.
52. Czychoł G., Phys. Rep., 1986, **143**, 277–345, doi:10.1016/0370-1573(86)90177-8.
53. Hanke W., Hirsch J.E., Phys. Rev. B, 1982, **25**, 6748, doi:10.1103/PhysRevB.25.6748.
54. Farkašovský P., Z. Phys. B, 1997, **104**, 553, doi:10.1007/s002570050489.

Дослідження конденсації екситонів методом DMRG для узагальненої моделі Фалікова-Кімбала

П. Фаркашовський

Інститут експериментальної фізики, Словацька академія наук, вул. Ватсонова 47, Кошиці, Словаччина

Формування і конденсація зв'язаних екситонних станів між електронами з зони провідності та дірками з валентної зони, безумовно, належить до однієї з найбільш захоплюючих ідей сучасної фізики твердого тіла. У цьому короткому огляді, ми представляємо останній прогрес у цій галузі, що був досягнутий завдяки розрахункам методом ренорм групи матриці густини (DMRG) для різних узагальнень моделі Фалікова-Кімбала. Особлива увага приділяється опису найважливіших механізмів (взаємодій), які впливають на стабільність екситонної фази, а саме: (i) міжзонна d - f кулонівська взаємодія, (ii) перенос f -електронів, (iii) парна і непарна нелокальна гібридизація, (iv) комбіновані ефекти локальної та нелокальної гібридизації, (v) кулонівська взаємодія найближчих сусідів між d - і f -електронами та (vi) корельований перенос. Широко обговорюється відповідність числових результатів, отриманих для різних узагальнень моделі Фалікова-Кімбала, для опису реальних d - f матеріалів.

Ключові слова: модель Фалікова-Кімбала, квантові конденсати, одновимірні системи
